Available online at www.sciencedirect.com
ScienceDirect
Optics Communications 281 (2008) 626–632
OPTICS COMMUNICATIONS
www.elsevier.com/locate/optcom

Optogalvanic detection of velocity-selective optical pumping in an open, cascade atomic medium

Luís E.E. de Araujo [a,*], Silvânia A. Carvalho [a], Luciano S. Cruz [a], A.A. Soares [a], Armando Mirage [b], Daniel Pereira [a], Flavio C. Cruz [a]

[a] *Instituto de Física "Gleb Wataghin", Universidade Estadual de Campinas, Campinas, SP 13083-970, Brazil*
[b] *Instituto de Pesquisas Energéticas e Nucleares, C. Postal 11049, São Paulo, SP 05422-970, Brazil*

Received 28 August 2007; received in revised form 16 October 2007; accepted 17 October 2007

Abstract

We performed two-color spectroscopy of the $(4s^2)\ ^1S_0 \rightarrow (4s4p)\ ^1P_1 \rightarrow (4p^2)\ ^1D_2$ calcium atomic transition and observed velocity-selective optical pumping in a calcium hollow cathode lamp by means of optogalvanic detection. The optical pumping signature in optogalvanic detection is compared to that of fluorescence and transmission detections. The optogalvanic technique is found to be a very sensitive method of detecting optical pumping and could be used in distinguishing optical pumping from electromagnetically induced transparency.

Keywords: Optogalvanic detection; Velocity-selective optical pumping; Electromagnetically induced transparency

Optogalvanic detection is a well-established and powerful technique of laser spectroscopy [1]. The optogalvanic method is a highly sensitive technique for detecting atomic population changes induced by light absorption. It is based on detecting an impedance change in a gas discharge whenever an optical transition is excited in the atoms embedded in the discharge. It has thus been successfully applied, for example, in Doppler-free spectroscopy [2–4], two-photon spectroscopy [5,6], velocity-changing-collision studies [7], wavelength calibration [8], laser frequency stabilization [9], and optical pumping detection [10]. In previous work [4], some of the authors performed high-resolution (sub-Doppler) and high-sensitivity saturated spectroscopy in a calcium hollow-cathode lamp (HCL) by means of the optogalvanic effect.

Alkaline-earth atoms, such as calcium, have been receiving increasing attention in the last years due to their applications in optical atomic clocks [11,12], ultracold collisions [13], and Bose–Einstein condensation [14]. These helium-like elements lack hyperfine structure, and can offer nearly ideal approximations to truly closed two- and three-level systems.

In this article, we report a two-color spectroscopy study of the $(4s^2)\ ^1S_0 \rightarrow (4s4p)\ ^1P_1 \rightarrow (4p^2)\ ^1D_2$ calcium transition in a gas of neutral calcium atoms embedded into a krypton-gas electrical discharge produced by an HCL. We describe the experimental observation of velocity-selective optical pumping via optogalvanic detection. This study was motivated by a search of suitable three-level transitions to be used in implementing a two-photon, laser-cooling scheme for calcium atoms [15], as well as of transitions appropriate for the observation of electromagnetically induced transparency (EIT) [16] in calcium HCLs. We compare the nonoptical (optogalvanic) absorption signal of a probe beam against optical (fluorescence and transmission) absorption signals. The optical signals observed are very similar to those associated with EIT, and we show that optogalvanic detection could be an effective tool in distinguishing optical pumping from EIT, particularly when the excitation fields are strong. We find the optogalvanic

* Corresponding author. Tel.: +55 19 3521 5405; fax: +55 29 3521 5427.
E-mail addresses: araujo@ifi.unicamp.br (L.E.E. de Araujo), flavio@ifi.unicamp.br (F.C. Cruz).

0030-4018/$ - see front matter © 2007 Elsevier B.V. All rights reserved.
doi:10.1016/j.optcom.2007.10.041

technique to be a very sensitive method to observe optical pumping.

The investigated atomic system is shown in Fig. 1(a) and consists of an open, three-level cascade atomic system excited by two counterpropagating, strong laser beams. A probe field is scanned across the $(4s^2)\ {}^1S_0 \rightarrow (4s4p)\ {}^1P_1$ transition in the presence of a coupling field resonant with the $(4s4p)\ {}^1P_1 \rightarrow (4p^2)\ {}^1D_2$ transition. The probe transition is centered at $\lambda_p = 423$ nm and is commonly used for laser-cooling of calcium. The coupling transition is at $\lambda_c = 586$ nm. The intermediate $(4s4p)\ {}^1P_1$ state has a high natural decay rate of $\gamma_1 = 2\pi \times 34$ MHz and a homogeneous saturation intensity of approximately 60 mW/cm^2. The uppermost $(4p^2)\ {}^1D_2$ state decays to the intermediate $(4s4p)\ {}^1P_1$ state at a rate of $\gamma_2 = 2\pi \times 11$ MHz, and it also decays to the $(4s5p)\ {}^1P_1$ state (not shown in the figure) at a rate $\gamma_3 = 2\pi \times 0.18$ MHz [17]. The $(4s5p)\ {}^1P_1$ state, in turn, decays to the metastable $(3d4s)\ {}^1D_2$ state (also not shown), which has a lifetime much longer than the diffusion time of the atoms out of the laser beams, turning this into an open system.

Fig. 1(b) shows the experimental setup. Two laser beams, both with a 3.0-mm diameter, enter the HCL counterpropagating to each other. The lasers have orthogonal polarizations and spatially overlap throughout the extension of the lamp. The blue laser is obtained from a frequency-doubled, home-built Ti-Sapphire laser, which delivers up to 16 mW of blue light at the entrance to the lamp, with a linewidth of approximately 1 MHz. The yellow laser is from a Coherent 699 ring-dye laser, with up to 150 mW at 586 nm (and less than a 1 MHz linewidth) at the lamp.

The calcium atomic vapor is created by sputtering induced by a direct-current hollow-cathode discharge (120 V, 100 mA). Our HCL is a home-built lamp [4] filled with krypton-gas at 2.0 torr. It is 26-cm long and made of Pyrex glass with optical windows. Two ring titanium anodes are placed 0.5 cm on each side of a 20-mm long, cylindrical steel cathode where a small calcium tube (3-mm bore) is inserted. The optical density can be easily changed by varying the lamp current, going from an optically thin to a very thick medium for the blue probe beam. At 30 mA, the Ca atomic density is on the order of 10^{10} cm^{-3}. Typical Doppler widths (full width at half maximum, FWHM) range from 1.3 to 2.2 GHz, corresponding to temperatures from 750 to 1200 K [4]. With no lasers present, most calcium atoms are in their ground state. Collisions with electrons or ions populate the excited states and also ionize both sputtered and buffer gas atoms. Numerous other direct and indirect collision mechanisms also contribute to ionization. Upon laser excitation, these ionization processes are perturbed, and the impedance of the discharge is changed, generating an optogalvanic signal [1].

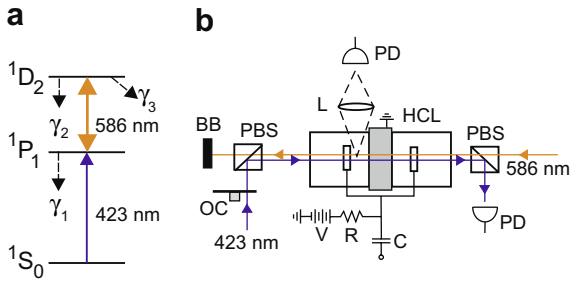

Fig. 1. (a) The open, three-level-cascade Ca system. Population may leak out of the system through the $^1D_2$ state. (b) The experimental setup: PD, photodetectors; PBS, polarizing beam splitters; OC, optical chopper; L, lens; V, power supply; R, ballast resistor; C, capacitor; BB, beam block; and HCL, hollow cathode lamp. The gray rectangle in the middle of the HCL is the cathode, and the two small rectangles symmetrically placed by its sides are the anodes. The counterpropagating beams were displaced in the figure for better viewing.

In the setup of Fig. 1b, absorption of the probe laser beam is detected in three different ways: an optogalvanic signal is detected by measuring the voltage across the electrodes; transmission of the blue laser through the HCL is monitored by a photodetector; and fluorescence from the region in the lamp between the first (left) anode and the cathode is imaged by a lens into another photodetector. The blue laser is amplitude modulated by an optical chopper at 2 kHz, and the optogalvanic, transmission and fluorescence signals are detected by three independent lock-in amplifiers. For spectroscopic purposes, both excitation beams would be modulated, and the combined effect of the two beams detected. We want to look at absorption of the probe beam alone, and thus, only this one beam is modulated.

Fig. 2a shows typical absorption spectra of the blue beam (transmission, fluorescence and optogalvanic signals) as a function of its detuning from the intermediate $^1P_1$ state taken at a lamp current of 10 mA. The yellow coupling beam was fixed on resonance. The intensity in the blue and yellow lasers were 37 mW/cm^2 (Rabi frequency $\alpha \approx 0.28\gamma_1$) and 707 mW/cm^2 ($\Omega \approx 1.15\gamma_1$), respectively. At 10 mA, the lamp is optically thick for the probe blue beam. A strong absorption occurs as the laser is tuned toward resonance, and its transmission decreases. However, close to resonance, a small increase in the probe's transmission is detected. Simultaneously, the fluorescence emitted from the lamp decreases at zero detuning of the probe beam. Both signals indicate a decrease in absorption of the probe blue beam. At a higher probe intensity (140 mW/cm^2, or $\alpha \approx 0.54\gamma_1$), absorption of the probe beam is further decreased on resonance, as shown in Fig. 2b. Since the atomic system is open and the excitation beams are strong, population is optically pumped from the ground $^1S_0$ state to the metastable $^1D_2$ state, and then out of the system. A significant change in the optogalvanic signal is also seen on resonance for the two cases of probe intensities, but with a distinction: Both the fluorescence and transmission signals reverse direction as the probe beam reaches resonance, but the optogalvanic signal does not. In the optogalvanic signal for this particular transition, optical pumping is

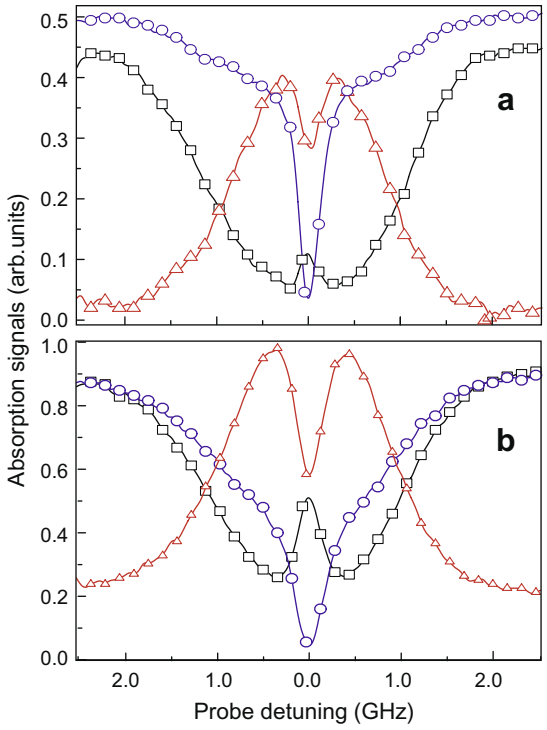

Fig. 2. The optogalvanic (blue ○), transmission (black □) and fluorescence (red △) absorption signals taken with 707 mW/cm^2 ($\Omega \approx 1.15\gamma_1$) of coupling intensity and (a) 37 mW/cm^2 ($\alpha \approx 0.283\gamma_1$) and (b) 140 mW/cm^2 ($\alpha \approx 0.54\gamma_1$) of probe intensity. Both the fluorescence and optogalvanic signals were vertically shifted by an arbitrary amount for better viewing. Both signals go to zero only far off-resonance. (For interpretation of the references to color in this figure legend, the reader is referred to the web version of this article.)

characterized by a further decrease in the voltage drop across the electrodes, and correspondingly, in the HCL's impedance. Naively, one could expect the amplitude of the optogalvanic signal to decrease as the absorption of the probe beam decreases, but we observe the opposite behavior.

We determined the width of the optical pumping resonances by fitting the sum of a Doppler and a Lorentzian profiles to the absorption curves of Fig. 2a. The optical pumping resonances thus found have different widths: 379 MHz, 257 MHz, and 233 MHz for the optogalvanic, fluorescence and transmission signals, respectively, measured at their FWHM. The main reason for this difference is that these signals monitor absorption over different lengths in the HCL. The transmission signal corresponds to absorption over the entire length of the lamp; the optogalvanic signal reflects the absorption across the two anodes; and the fluorescence signal gives the absorption between the first anode and the cathode. The complexity of the optogalvanic generation further contributes to differentiate the optical pumping width in the optogalvanic signal from those in the optical signals. At 10 mA, the lamp is optically thick for the blue probe beam. At much lower currents, corresponding to an optically thinner medium, we observed approximately the same width in the three signals. In all three cases, the optical pumping resonances are sub-Doppler due to the velocity-selective nature of the excitation.

By detuning the coupling laser from resonance, different atomic velocity classes can be selected, and optical pumping occurs at a probe detuning different from zero. As can be seen in Fig. 3, the optogalvanic signal exhibits this dependence on coupling detuning. Since the coupling and probe beams are significantly wavelength mismatched, the residual Doppler broadening $|k_p - k_c|u$, where $k_{p,c}$ is the probe (coupling) wave number and u is the most probable atomic velocity, is very large: approximately $2\pi \times 245$ MHz, or $\approx 7.2\gamma_1$. Thus, only a very small fraction of the atoms participate in an off-resonance step-wise excitation, even with strong beams [18]. For a very large coupling detuning,

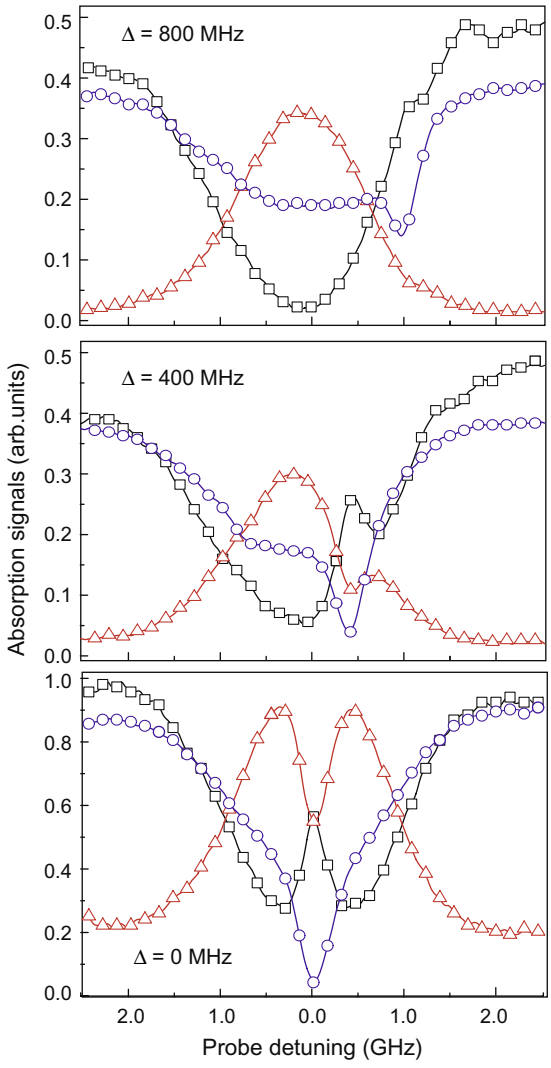

Fig. 3. The optogalvanic (blue ○), transmission (black □) and fluorescence (red △) absorption signals for three different detunings Δ of the coupling laser. The probe and coupling intensities were 170 mW/cm^2 ($\alpha \approx 0.60\gamma_1$) and 1061 mW/cm^2 ($\Omega \approx 1.41\gamma_1$), respectively. Both the fluorescence and optogalvanic signals were vertically shifted by an arbitrary amount for better viewing. (For interpretation of the references to color in this figure legend, the reader is referred to the web version of this article.)

the optical pumping signature in the fluorescence and transmission signals vanishes, but a clear signature remains in the optogalvanic signal. Optogalvanic detection is thus a quite sensitive technique for detecting very small levels of optical pumping.

Fig. 4 shows the three absorption signals taken at a higher lamp current (50 mA) at which the atomic medium is optically much denser; no probe light is transmitted in this case, even in the presence of the strong coupling laser. Still, some of the blue laser can propagate past the first anode, and a fluorescence signal is observable. At this higher current, the lineshape of the optogalvanic spectrum has changed considerably as a consequence of the atomic medium being optically very thick. Because the optogalvanic signal is a measure of the impedance change only in the region between the two anodes and the cathode, the probe laser's Doppler spectrum (in the absence of the coupling laser) shows a broad flat region on its profile just because absorption is stronger at the center and weaker at the wings of the spectrum. Near the line center, the probe laser can be completely absorbed before reaching the electrodes, while it still reaches the region between the electrodes at the wings of the Doppler profile. Therefore, this Doppler optogalvanic spectrum appears to show two side lobes at approximately ± 1.5 GHz. When the coupling laser is present, a large dip appears at zero detuning. Optical pumping has a dramatic effect on the optogalvanic signal in a very thick medium.

With both beams on resonance, a bright yellow fluorescence is emitted from the HCL. Fig. 5a shows the detected yellow fluorescence. Here, the blue probe laser is kept fixed on resonance, while the yellow coupling laser is scanned across the (4s4p) $^1P_1 \rightarrow (4p^2)\ ^1D_2$ transition. As indicated by the fluorescence signal, population in the uppermost excited state increases when both lasers are tuned to resonance. To measure an optogalvanic signal from the yellow laser, we moved the optical chopper from the path of the blue laser to that of the yellow laser. The solid line in Fig. 5b shows the optogalvanic signal generated by the coupling yellow beam in the absence of the probe blue laser. Such an optogalvanic signal can be obtained because collisions of calcium atoms with fast electrons and ions weakly populate the intermediate (4s4p) $^1P_1$ state. The optogalvanic signal shows a wide (1.8 GHz) Doppler absorption profile. But when the probe blue laser is present, a much larger and narrower resonance (dashed line) is seen in the optogalvanic signal. The peak of this resonance is 80 times larger than that of the Doppler profile when the blue laser is not present. Its width is also significantly smaller: 340 MHz. In this case, because the probe laser is fixed on resonance, the coupling resonance is observed without a Doppler background in the optogalvanic signal, even for a large coupling intensity. For this transition, the optogalvanic signal has opposite polarity with respect to the one shown in Fig. 2, and its amplitude increases along with the fluorescence as the coupling laser

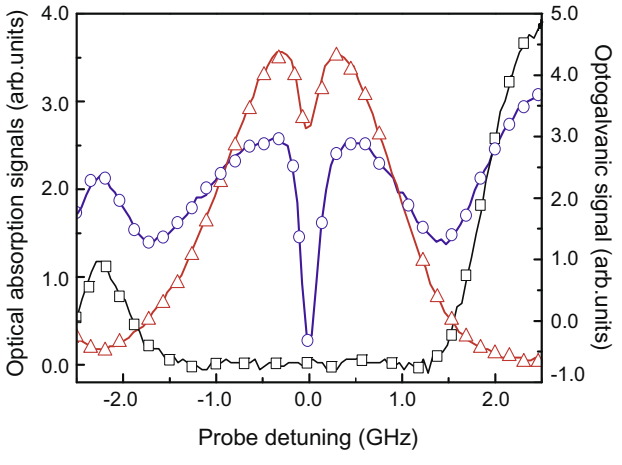

Fig. 4. The optogalvanic (blue ○), transmission (black □) and fluorescence (red △) signals for an HCL current of 50 mA taken with a coupling intensity of 707 mW/cm^2 ($\Omega \approx 1.15\gamma_1$) and probe intensity of 85 mW/cm^2 ($\alpha \approx 0.42\gamma_1$). Both the fluorescence and optogalvanic signals were vertically shifted by an arbitrary amount for better viewing. (For interpretation of the references to color in this figure legend, the reader is referred to the web version of this article.)

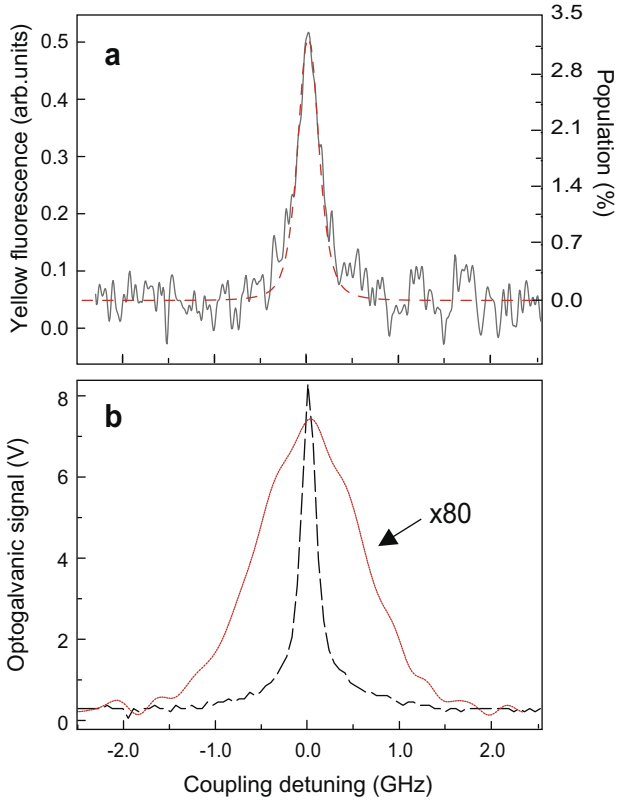

Fig. 5. (a) The detected yellow fluorescence signal (solid gray line) and the calculated population in the uppermost excited $^1D_2$ state (dashed red line). (b) The optogalvanic signal generated by the coupling yellow laser with (dashed black line) and without (solid red line) the probe blue laser. In both (a) and (b), the experimental coupling intensity was 707 mW/cm^2 ($\Omega \approx 1.5\gamma_1$) and the probe intensity was 113 mW/cm^2 ($\alpha \approx 0.49\gamma_1$); the numerical parameters are those of Fig. 6. (For interpretation of the references to color in this figure legend, the reader is referred to the web version of this article.)

is tuned to resonance. Both signals indicate an increase in absorption of the coupling laser.

An increase in probe transmission and decrease in fluorescence similar to those of Fig. 2 can also result from destructive quantum interferences of the kind associated with EIT. When the excitation beams are strong, the EIT resonance can be power broadened. In such cases, experimentally distinguishing EIT from optical pumping may be difficult. However, whenever the excitation lasers are very mismatched, and the coupling wavelength λ_c is longer than the probe wavelength λ_p, as it is in our case, EIT is very difficult to observe in a Doppler broadened medium [19]. Furthermore, since in the EIT case most of the atomic population should be trapped in the ground state, the observed yellow fluorescence strongly suggests that optical pumping is indeed the physical mechanism responsible for our observations.

Velocity-changing-collisions (VCC) with a buffer gas are well known to limit the resolution in sub-Doppler spectroscopy in HCLs [20]. They are also known to affect optical pumping by shuffling atoms between different velocity classes, and therefore, into and out of resonance with the optical beams. In three-level Λ systems, the combination of optical pumping and VCC has been shown to effectively polarize atomic vapors [21]. And in cascade systems, experiments by Bjokholm, Liao and Wokaun [22] showed that VCC can significantly reduce the effects of velocity-selective optical pumping.

To determine the influence of VCC in our observations, we numerically solved the semiclassical Bloch equations for the density matrix elements in the steady state regime. Usually the effects of VCC are modeled by considering that for the diagonal elements of the density matrix, collisions result in velocity changes and a redistribution of atomic population among the different velocity classes:

$$\left[\frac{\partial}{\partial t}\rho_{ii}(v,t)\right]_{\text{coll}} = -\Gamma_{ii}(v)\rho_{ii}(v,t) + \int \mathrm{d}v' W_{ii}(v' \to v)\rho_{ii}(v',t), \tag{1}$$

where $W_{ii}(v' \to v)$ is the collision kernel, and $\Gamma_{ii}(v) = \int W_{ii}(v' \to v)\mathrm{d}v'$ is the rate of VCC. The first term in the right hand side of the above equation represents the population that is being removed from velocity class v by collisions; the second term represents the population that is being brought into the same velocity class v, from other classes, by collisions. Since the atomic system consists of different electronic states of the atom, for the off-diagonal elements, collisions are "phase-interrupting" [23]:

$$\left[\frac{\partial}{\partial t}\rho_{ij}(v,t)\right]_{\text{coll}} = -\gamma_{ij}^{c}\rho_{ij}(v,t), \tag{2}$$

where γ_{ij}^{c} is a homogeneous collisional-broadening rate.

Strong VCC, corresponding to velocity thermalization within only a few collisions, can occur whenever the mass ratio of the active atom to the perturber atom is less than or equal to one [24]. In our case, this ratio is $m_{Ca}/m_{Kr} \approx 0.48$. In the limit of strong collisions, the probability of an atom having a particular velocity after a collision is independent of its previous velocity [21]. Thus one can write $W_{ii}(v' \to v) \approx W(v) = \Gamma_0 f(v)$, where $f(v) = \exp(-v^2/u^2)/(\sqrt{\pi}u)$ is the Maxwell–Boltzman velocity distribution with $u = \sqrt{2k_B T/m}$ being the most probable atomic velocity.

The semiclassical Bloch equations describing the interaction of the driving lasers with the atoms are then:

$$\begin{aligned}
\dot{\rho}_{bb} &= -0.5i\alpha(\rho_{ab} - \rho_{ba}) + \gamma_1\rho_{aa} - \Gamma_0\rho_{bb} \\
&\quad + \int W(v')\rho_{bb}(v')\mathrm{d}v' - (r_a + r_b)\rho_{bb} - r[\rho_{bb} - \rho_{bb}^0], \\
\dot{\rho}_{aa} &= -0.5i\Omega(\rho_{ca} - \rho_{ac}) - 0.5i\alpha(\rho_{ba} - \rho_{ab}) - \gamma_1\rho_{aa} \\
&\quad + \gamma_2\rho_{cc} - \Gamma_0\rho_{aa} + \int W(v')\rho_{aa}(v')\mathrm{d}v' + r_a\rho_{bb} - r\rho_{aa}, \\
\dot{\rho}_{cc} &= -0.5i\Omega(\rho_{ac} - \rho_{ac}) - \gamma_2\rho_{ac} - \gamma_3\rho_{ac} - \Gamma_0\rho_{cc} \\
&\quad + \int W(v')\rho_{ac}(v')dv' + r_c\rho_{bb} - r\rho_{ac}, \\
\dot{\rho}_{ab} &= -\Gamma_{ab}\rho_{ab} - 0.5i\alpha(\rho_{bb} - \rho_{aa}) - 0.5i\Omega\rho_{cb} - r\rho_{ab} - \gamma_{ab}^{c}\rho_{ab}, \\
\dot{\rho}_{ca} &= -\Gamma_{ca}\rho_{ca} - 0.5i\Omega(\rho_{aa} - \rho_{cc}) - 0.5i\alpha\rho_{cb} - r\rho_{ca} - \gamma_{ca}^{c}\rho_{ca}, \\
\dot{\rho}_{cb} &= -\Gamma_{cb}\rho_{cb} - 0.5i\Omega\rho_{ab} + 0.5i\alpha\rho_{ca} - r\rho_{cb} - \gamma_{cb}^{c}\rho_{cb}.
\end{aligned} \tag{3}$$

Here, state a corresponds to the intermediate excited $^1P_1$ level, b to the ground $^1S_0$ level, and c to the uppermost excited $^1D_2$ level. $\Gamma_{ab} = \gamma_1/2 + i(\delta + \vec{k}_p \cdot \vec{v})$, $\Gamma_{ca} = (\gamma_1 + \gamma_2 + \gamma_3)/2 + i(\Delta + \vec{k}_c \cdot \vec{v})$, and $\Gamma_{cb} = (\gamma_2 + \gamma_3)/2 + i[(\delta + \Delta) + (\vec{k}_p + \vec{k}_c) \cdot \vec{v}]$; $\delta = \omega_{ba} - \omega_p$ is the detuning of the probe laser from resonance, and $\Delta \equiv 0$ is that of the coupling laser; $\vec{k}_p$ and $\vec{k}_c$ are the wave vectors of the probe and coupling lasers, respectively. (γ_1, γ_2, and γ_3 are as defined previously). We assumed a Doppler linewidth of 1.8 GHz, corresponding to $k_p\, u = 26\gamma_1$. In an HCL, due to collisions of the neutral Ca atoms with energetic electrons and ions, the excited atomic states are weakly populated even in the absence of any laser beams. The incoherent pumping rates r_a and r_c at which population is transferred to states a and c, respectively, by these collisions have not been determined for our lamp. We have arbitrarily set these rates to $r_a = r_c = 2\pi \times 3.4$ kHz, but they are typically much smaller than this value [7]. For the laser beams employed in our experiment, the atoms have an estimated diffusion rate out of the laser beams of $r = 2\pi \times 34$ kHz that is much faster than the decay rate of the metastable (3d4s) $^1D_2$ state:$2\pi \times 6$ Hz. The Rabi frequency of the probe and coupling lasers are $\alpha = 2\mu_{ab}\, E_p/\hbar$ and $\Omega = 2\mu_{ca}\, E_c/\hbar$, respectively. In the absence of collisions, and with no lasers applied, the atoms are distributed in the ground state across the different velocity classes according to $\rho_{bb}^0(v) = f(v)$.

The intermediate state population of the Doppler-broadened atomic system is found by velocity integrating element $\rho_{aa}(v)$ of the density matrix:

$$P_{aa}(\delta) = \int_{-\infty}^{\infty} \rho_{aa}(v,\delta)\mathrm{d}v. \quad (4)$$

By using the known values for the decay rates and wavelengths, and adjusting the Rabi frequencies and collisional rates (γ_{ij}^{c} and Γ_0), we could reproduce the experimental results as shown in Fig. 6. The solid line in Fig. 6 shows the calculated population P_{aa} in the intermediate $^1P_1$ state as a function of probe detuning. A decrease in population is seen on resonance, and agreement with the experiment is good. The linewidth of the calculated spectrum is close to that of the experiment. However, the calculations reproduced the experimental results only by setting the collisional rates to zero. Even a small VCC rate of $\Gamma_0 = 0.2\gamma_1$, significantly decreases the dip in the population spectrum. Surprisingly, VCC appear to play no role on our observations.

If we set $\gamma_3 = 0$ in the model, and thus close our atomic system, the population dip is strongly reduced as shown in Fig. 6. Thus the very small open character ($\gamma_3 = 0.005\gamma_1$) of the atomic system is sufficient to significantly change the absorption of the probe laser beam. Further theoretical evidence toward optical pumping was given by calculating the intermediate state population through rate equations. By solving the rate equations for the open atomic system we were also able to reproduce the experimental results, thus showing that the atomic coherences have no significant influence on the results. And finally, we also calculated the population in the uppermost excited state c ($^1D_2$). The dashed red line in Fig. 5a shows this calculated population. It also compares favorably with the experimental result, ruling out EIT as responsible for the decrease in absorption of the probe beam.

Modeling of the optogalvanic signal itself is very difficult due to several simultaneous effects that happen in the HCL. However, its behavior under optical pumping can be understood qualitatively in the following way. The optogalvanic signal is a measure of the total impedance of the lamp, and therefore, a measure of how easy it is to ionize the neutral atoms. Whenever light is absorbed, population is moved to higher energy levels, closer to ionization. When both probe and coupling lasers are on resonance, absorption of the probe laser may be reduced, but population is still transferred to the uppermost excited state, making it easier to ionize the atom through collisions with energetic electrons and other ions. Thus, the amplitude of the optogalvanic signal generated by the probe laser increases while the probe absorption decreases.

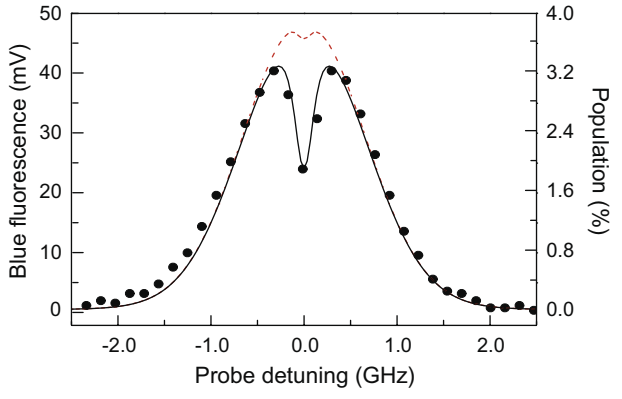

Fig. 6. The detected blue fluorescence signal (solid circles) from Fig. 2(b) and the calculated intermediate-state population (solid black line) as a function of probe detuning. The adjusted Rabi frequencies are $\alpha = 1.0\gamma_1$ and $\Omega = 2.0\gamma_1$. The dashed red line shows the calculated population for a closed system: $\gamma_3 = 0$. (For interpretation of the references to color in this figure legend, the reader is referred to the web version of this article.)

In conclusion, we observed velocity-selective optical pumping in an open cascade system by means of the optogalvanic signal generated in a calcium hollow cathode lamp. The optical pumping signature consists of an amplitude increase of the optogalvanic signal, although absorption of the laser generating the signal decreases. This behavior can be qualitatively explained by the population increase in the uppermost excited state of the cascade system, which makes ionization by collisions easier. By choosing an atomic level system more appropriate than the one investigated here (for example, one for which the probe and coupling wavelength are more closely matched, which reduces the residual Doppler broadening), it should be possible to use optogalvanic detection to monitor the occurrence of EIT. That is, it should be possible to detect a change in the impedance of a gas discharge as a result of quantum interferences. Experimentally distinguishing optical pumping from EIT in an optical signal may be difficult, particularly when strong beams are employed, since the optical signals (fluorescence and transmission) are very similar in both cases. The nonoptical optogalvanic signal may be used to differentiate the two effects. In EIT, most of the atomic population remains trapped in the ground state, and the optogalvanic signal should decrease on resonance. As shown here, in optical pumping, the optogalvanic signal increases on resonance. Optogalvanic detection might also be very convenient for observing quantum-interference related phenomena in weak transitions for which optical detection is difficult, such as the $^1S_0 \rightarrow {}^3P_1^0$ intercombination "clock" transition in alkaline-earth atoms (374 Hz linewidth for Ca).

Acknowledgements

The authors acknowledge the financial support of FAPESP, CNPq and CAPES.

References

[1] B. Barbieri, N. Beverini, A. Sasso, Rev. Mod. Phys. 62 (1990) 603.
[2] J.E. Lawler, A.I. Ferguson, J.E.M. Goldsmith, et al., Phys. Rev. Lett. 42 (1979) 1046.
[3] D.J. Jackson, H. Gerhardt, T.W. Hansch, Opt. Commun. 37 (1981) 23.
[4] R.L. Cavasso-Filho, A. Mirage, A. Scalabrin, D. Pereira, F.C. Cruz, J. Opt. Soc. Am. B 18 (2001) 1922.
[5] J.E.M. Smith, A.I. Ferguson, J.E. Lawler, A.L. Schawlow, Opt. Lett. 4 (1979) 230.

[6] H. Wakata, S. Saikan, M. Kimura, Opt. Commun. 38 (1981) 271.
[7] W.H. Richardson, L. Maleki, E. Garmire, Phys. Rev. A 36 (1987) 5713.
[8] D.S. King, P.K. Schench, K.C. Smyth, J.C. Travis, Appl. Opt. 16 (1977) 2617.
[9] S. Yamaguchi, M. Suzuki, Appl. Phys. Lett. 41 (1982) 597.
[10] L. Julien, M. Pinard, J. Phys. B: At. Mol. Phys. 15 (1982) 2881.
[11] C. Degenhardt, H. Stoehr, C. Lisdat, et al., Phys. Rev. A 72 (2005) 062111.
[12] G. Wilpers, C.W. Oates, L. Hollberg, Appl. Phys. B 85 (2006) 31.
[13] S.B. Nagel, P.G. Mickelson, A.D. Saenz, et al., Phys. Rev. Lett. 94 (2005) 083004.
[14] Y. Takasu, K. Maki, K. Komori, et al., Phys. Rev. Lett. 91 (2003) 040404.
[15] W.C. Magno, R.L. Cavasso, F.C. Cruz, Phys. Rev. A 67 (2003) 043407.
[16] M. Fleischhauer, A. Imamoglu, J.P. Marangos, Rev. Mod. Phys. 77 (2005) 633.
[17] N. Vaek, M. Godefroid, J.E. Hansen, J. Phys. B: At. Mol. Opt. Phys. 24 (1991) 361.
[18] R. Salomaa, J. Phys. B: At. Mol. Opt. Phys. 10 (1977) 3005.
[19] J.R. Boon, E. Zekou, D. McGloin, M.H. Dunn, Phys. Rev. A 59 (1999) 4675.
[20] F.C. Cruz, A. Mirage, A. Scalabrin, D. Pereira, J. Phys. B: At. Mol. Opt. Phys. 27 (1994) 5851.
[21] W.W. Quivers Jr., Phys. Rev. A 34 (1986) 3822.
[22] J.E. Bjorkholm, P.F. Liao, A. Wokaun, Phys. Rev. A 26 (1982) 2643.
[23] P.R. Berman, Phys. Rev. A 13 (1976) 2191.
[24] P.F. Liao, J.E. Bjorkholm, P.R. Berman, Phys. Rev. A 21 (1980) 1927.